Depletion force between two large spheres suspended in a bath of small spheres: Onset of the Derjaguin limit

M. Oettel
Max-Planck-Institut für Metallforschung, Heisenbergstrasse 3, 70569 Stuttgart and Institut für Theoretische und Angewandte Physik, Universität Stuttgart, Pfaffenwaldring 57, 70569 Stuttgart, Germany
(Received 22 October 2003; published 29 April 2004)

We analyze the depletion interaction between two hard colloids in a hard-sphere solvent and pay special attention to the limit of large size ratio between colloids and solvent particles which is governed by the well-known Derjaguin approximation. For separations between the colloids of less than the diameter of the solvent particles (defining the depletion region), the solvent structure between the colloids can be analyzed in terms of an effective two-dimensional gas. Thereby we find that the Derjaguin limit is approached more slowly than previously thought. This analysis is in good agreement with simulation data which are available for a moderate size ratio of 10. Small discrepancies in results from density functional theory (DFT) at this size ratio become amplified for larger size ratios. Therefore we have improved upon previous DFT techniques by imposing test-particle consistency which connects DFT to integral equations. However, the improved results show no convergence towards the Derjaguin limit and thus we conclude that this implementation of DFT together with previous ones which rely on test-particle insertion become unreliable in predicting the force in the depletion region for size ratios larger than 10.

DOI: 10.1103/PhysRevE.69.041404 PACS number(s): 83.80.Hj, 05.20.Jj

I. INTRODUCTION AND PHYSICAL PROBLEM

The stability of mixtures containing large colloidal particles in a solvent is determined by the effective interaction between the colloids. This effective interaction is a sum of the direct intercolloidal potential and, by the way of integrating out the solvent degrees of freedom, effective interaction terms. In the circumstances where colloidal and solvent interact mainly through hard-body-like potentials this effective interaction is largely determined by entropic effects, i.e., by the free volume which is accessible to the solvent particles. Therefore studies of idealized hard-body models may give important insights into the behavior of actual experimental systems, and in view of the large size difference between colloids and solvent particles in many natural systems investigations of the limit where the size ratio between colloid and solvent particles becomes infinite are also of practical importance. On the other hand, the theoretical connection between (i) general results of the statistical mechanics for mixtures, (ii) practical calculational methods such as simulations and density functional theory (DFT) which often are reliable for smaller size ratios only, and (iii) macroscopic models designed for large size ratios is interesting in itself and in fact has motivated the present study.

Both colloidal and solvent particles are taken to be hard spheres with radii R_2 and $R_1=\sigma/2$, respectively. The effective colloidal interaction is purely entropic and arises mainly through the effect of a depletion zone between the colloids (for surface-to-surface minimal distances $z<\sigma$), which is inaccessible to the solvent particles.

For large size ratios $\alpha=R_2/R_1$, the force F_α in the depletion zone $z<\sigma$ between the colloids can be obtained by just using bulk and surface thermodynamics. This is the Derjaguin approximation (its derivation is presented in more detail below) which states

$$\frac{F_\alpha(z)}{\pi(R_1+R_2)}=p(z-\sigma)-2\gamma_\infty, \quad z\leqslant\sigma. \tag{1}$$

Here, p is the bulk pressure at density ρ of the small spheres and γ_∞ is the surface excess energy per unit area for small spheres of density ρ at a planar hard wall. In the following we call the latter a surface tension although for hard spheres γ_∞ is negative and surface tensions are usually associated with positive quantities. For both quantities quasi-exact expressions are available [1,2],

$$\frac{p}{\rho}=\frac{1+\eta+\eta^2-\eta^3}{(1-\eta)^3}, \tag{2}$$

$$\frac{\gamma_\infty}{\rho}=-\frac{\frac{3}{4}\eta\left(1+\frac{44}{35}\eta-\frac{4}{5}\eta^2\right)}{(1-\eta)^3}, \quad \eta=\frac{\pi}{6}\rho. \tag{3}$$

In obtaining these equations we have used reduced units defined by setting

$$\beta\left(=\frac{1}{k_BT}\right)=\sigma=1 \tag{4}$$

and we will do likewise in all the following considerations. (T is the absolute temperature and k_B is Boltzmann's constant.)

In recent years, progress has been made in calculating the depletion force in hard systems by other theoretical means, such as simulations [3,4], integral equations [4], and density functional theory (DFT) [5–7]. In a recent paper [8], Henderson reviews this analysis of depletion forces in hard fluids and points to a serious discrepancy between Derjaguin's analysis on the one hand and the various theoretical approaches/molecular dynamics simulations on the other

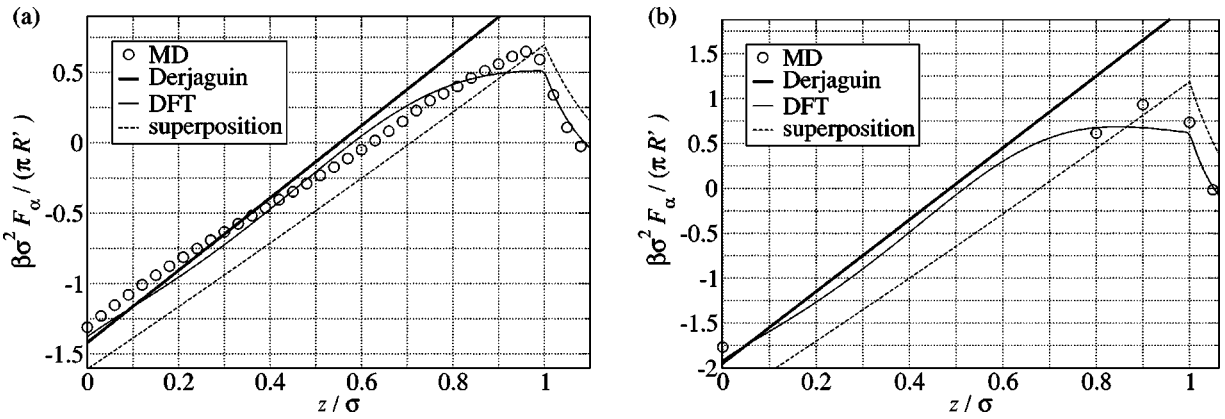

FIG. 1. A comparison between existing results for the force between two colloidal particles in the depletion region for the size ratio $\alpha=10$. Shown are results from molecular dynamics [3], DFT [5], the superposition approximation (using density profiles obtained as in Ref. [5]), and the Derjaguin limit for solvent densities: (a) $\rho=0.6$ and (b) $\rho=0.7$.

hand. Also there are some features of the density functional result which do not fit with the simulations either. These discrepancies had gone unnoticed partly due to the fact that comparisons were made between depletion *potentials* which add a fair amount of uncertainty to the simulation data since force curves with very few data points had to be integrated [3]. Also the limits inherent in the Derjaguin assumption have not been analyzed convincingly such that partial agreement versus disagreement with Derjaguin's result has not been taken seriously. Henderson's analysis concentrated on the depletion force between hard walls and hard colloids but applies equally well to the force between two colloids.

Before we analyze these discrepancies, we briefly present the strategies of the various approaches to obtain the depletion potential. Let us denote by $\rho(\mathbf{r};\mathbf{x}_1,\mathbf{x}_2)$ the density distribution of small spheres around two fixed hard spheres at positions $\mathbf{x}_1$ and $\mathbf{x}_2$. Then the depletion force on one big sphere can be obtained by summing over all small spheres the force between a single small sphere and the big sphere. By symmetry, the force will be directed along the axis joining the centers of the two big spheres and due to the hard sphere interactions the volume integral reduces to an integral over the surface of one big sphere. Its magnitude (negative for attraction, positive for repulsion) is given by

$$F_\alpha(z)=2\pi(R_1+R_2)^2\int_{-1}^{1} d(\cos\theta)\cos\theta\,\rho(\mathbf{r};\mathbf{0},\mathbf{x}_2)$$

$$[|\mathbf{r}|=R_1+R_2,\quad \mathbf{x}_2=(0,0,2R_2+z)]. \tag{5}$$

In simulations, just this formula is used. The superposition approximation also uses this formula and additionally assumes that $\rho(\mathbf{r};\mathbf{x}_1,\mathbf{x}_2)$ can be obtained by superimposing the two density distributions $\rho(\mathbf{r}-\mathbf{x}_i)$ around one fixed hard sphere centered at $\mathbf{x}_1$ and $\mathbf{x}_2$, respectively:

$$\rho(\mathbf{r};\mathbf{x}_1,\mathbf{x}_2)=\frac{1}{\rho}\rho(\mathbf{r}-\mathbf{x}_1)\rho(\mathbf{r}-\mathbf{x}_2). \tag{6}$$

The density distribution around one big sphere could be determined by, e.g., integral equation methods or by minimizing a density functional. When presenting superposition approximation results, we will use DFT results using the Rosenfeld functional (as originally given by Ref. [9]) as these are of superior quality. The DFT method of Ref. [5] also arrives at the depletion potential (whose derivative gives the depletion force) by just using the density distribution around one single big sphere but circumvents the crude approximation, Eq. (6), by making use of the potential distribution theorem (also known as Widom's insertion method). The method (which we call insertion route DFT) is explained in Appendix B. On the other hand, the distribution $\rho(\mathbf{r};\mathbf{x}_1,\mathbf{x}_2)$ could be obtained directly using DFT (in line with Ref. [5] we call this brute force DFT). It is numerically involved and only two studies exist in the literature, both for size ratios smaller than or equal to $\alpha=5$ [6,7]. Error bars on the results of Ref. [6] are much too large to arrive at a sensible conclusion. The much improved results of Ref. [7] indicate no significant deviation between the depletion potentials calculated using the insertion route and the brute force method, respectively.

For densities $\rho>0.5$ discrepancies between the above mentioned treatments and the simple Derjaguin formula become apparent as is illustrated in Fig. 1. For $\alpha=10$ and solvent sphere densities $\rho=0.6$ and 0.7 we show molecular dynamics (MD) data [3], Derjaguin's result, insertion route DFT data calculated as in Ref. [5], and data obtained from the superposition approximation. The deviation from Derjaguin's straight line is most obvious near $z=1$, i.e., near where just one small sphere fits between the two large spheres. The MD results seem to follow a straight line with a slope smaller than the one in Derjaguin's expression, p, but with a characteristic rounding off near $z=1$ which always overshoots the DFT data (see also Fig. 7 in Ref. [4] for another simulation). The DFT results show a flattening off which is characteristic for $\rho>0.5$ and $\alpha>10$. The same behavior is seen in results using bridge diagram corrected hypernetted chain (HNC) integral equations [4]. Finally, the superposition approximation produces a straight line with Derjaguin's slope but with a big offset. Using density distributions $\rho(\mathbf{r}-\mathbf{R})$ from less precise methods (integral equations with Percus-Yevick and Rogers-Young closure) offset

and slope of the straight line are changed considerably [3] such that these results fitted the MD data quite well. This led the authors of Ref. [3] to the erroneous conclusion that the superposition approximation is quite successful in predicting $\rho(\mathbf{r};\mathbf{x}_1,\mathbf{x}_2)$. From the present results, it is clear that the superposition approximation does not constitute a good model of the force in the depletion zone.

At first glance one is inclined to blame the discrepancies on the finiteness of α. After all, Derjaguin's result is supposed to be valid for $\alpha\to\infty$. Here the first problem arises: regarding this limit, Henderson gives an argument (which will be critically examined below) that deviations to Derjaguin should only occur for $z>1-1/(4R_1+4R_2)$ ($z>0.955$ for $\alpha=10$). This is clearly not the case for all results as can be seen in Fig. 1. Moreover the insertion route DFT results do not converge to the Derjaguin limit for higher α [5]. The second problem lies in the fact that Rosenfeld's (or related) DFT usually gives density distributions around fixed objects (wall [10], big spheres [11], wedge [12]) of such a high quality that they seem to parametrize MC/MD data also for higher densities, where MC denotes Monte Carlo. However, in the present case systematic discrepancies between the MD and the DFT results occur. A tentative first explanation why this happens lies in the possibility that insertion route and brute force DFT give substantially different results for $\alpha\geqslant 10$ (remember, there is no apparent difference for $\alpha=5$ [7]). A second possibility is that the higher-order correlations which are captured only approximately by any DFT model become more and more important. In fact, we will present below a picture for the depletion force which reveals quite subtle packing effects between the colloids which emerge for larger values of α.

There is an interesting consequence from all of this. Defining the depletion potential by

$$W_\alpha(z)=\int_z^\infty F_\alpha(z')dz', \tag{7}$$

we note that in the Derjaguin approximation $W_\alpha(0)<W_\alpha(1)$ only for $\rho<0.68$. Above that density, contact between the two big spheres is only a metastable minimum separated by a rather high potential barrier from the overall minimum which will be close to $z=1$. So, for higher densities the colloidal particles would not stick to each other. Although according to insertion route DFT $W_\alpha(0)-W_\alpha(1)$ also increases with increasing $\rho>0.7$, this quantity never changes its negative sign for physical densities (we checked this for $\alpha\leqslant 100$).

Therefore we can formulate our questions: Does the Derjaguin limit already set in for $\alpha\approx 10$? If not, why? What is the source of discrepancy between DFT and MD/MC? As Rosenfeld's DFT is now being used in studies of solvation forces for colloidal particles in liquids with interactions other than hard sphere [13], the understanding of its limits for hard spheres is crucial.

The remainder of the paper is organized as follows. In order to have a self-contained presentation, the Derjaguin limit for the depletion force is derived via (i) a force and (ii) energy analysis and (iii) exact relations from statistical mechanics. This section contains nothing new and leans heavily on the presentation in Ref. [8]. To shed light on the onset of the Derjaguin limit, we will rederive it in a slightly different way in the following section and thus show that it is not valid when the colloids are separated by $z\approx 1$. This will define the *annular slit approximation*. The depletion regime $z<1$ is then analyzed in terms of an effective two-dimensional system of small disks which builds up in the annular wedge between the colloids. Using scaled particle theory in two dimensions, we derive an expression for $F_\alpha(z)$ which for $\alpha\to\infty$ recovers the Derjaguin expression, although more slowly than Henderson anticipated.

For $\alpha=10$, the results of this analysis point to a flaw in the insertion route DFT treatment and show better agreement with the MD data. Therefore we will examine the insertion route DFT results closer and improve upon them by imposing test-particle consistency (see Appendix B). The equations obtained can also be viewed as reference HNC (RHNC) integral equations with the bridge diagrams calculated from the hard-sphere density functional. Therefore, results from any integral equation closure can be viewed as being akin to insertion route DFT calculations. The quality of the density functional is then closely related to the quality of the bridge function approximation.

Using test-particle consistent DFT, we find no convergence to Derjaguin's result for α up to 100 and an increasing difference to the annular slit approximation (which becomes more reliable for increasing ρ and α). With the premise that the Dejaguin limit is reached in a nonsingular way, we arrive therefore at the conclusion that insertion route DFT (and likewise integral equations) are unreliable for $\alpha>10$ since they miss some of the packing effects of the small spheres between the large colloids.

In the last section we briefly comment on the possibility that nonanalytic contributions might prevent a smooth transition to the Derjaguin limit.

II. DERJAGUIN APPROXIMATION

A. Force analysis

The geometrical arrangement of the two colloids is shown in Fig. 2. The boundary of the exclusion zone for the centers of the small particles is indicated by the dashed lines, thus the exclusion zone is two (possibly overlapping) spheres of radius $R'=R_1+R_2$. The depletion force between the two large spheres is obtained by summing local pressures over the area of one (exclusion) sphere,

$$F_\alpha(z)=2\pi R'^2\int_{-1}^{1} d(\cos\theta)p_{\mathrm{loc}}(\theta). \tag{8}$$

The Derjaguin approximation consists in replacing the local pressure by the solvation force per unit area of a planar slit with width l where the width refers to the minimal distance between the excluded volumes of the walls:

$$p_{\mathrm{loc}}(\theta)\approx f_\infty(l). \tag{9}$$

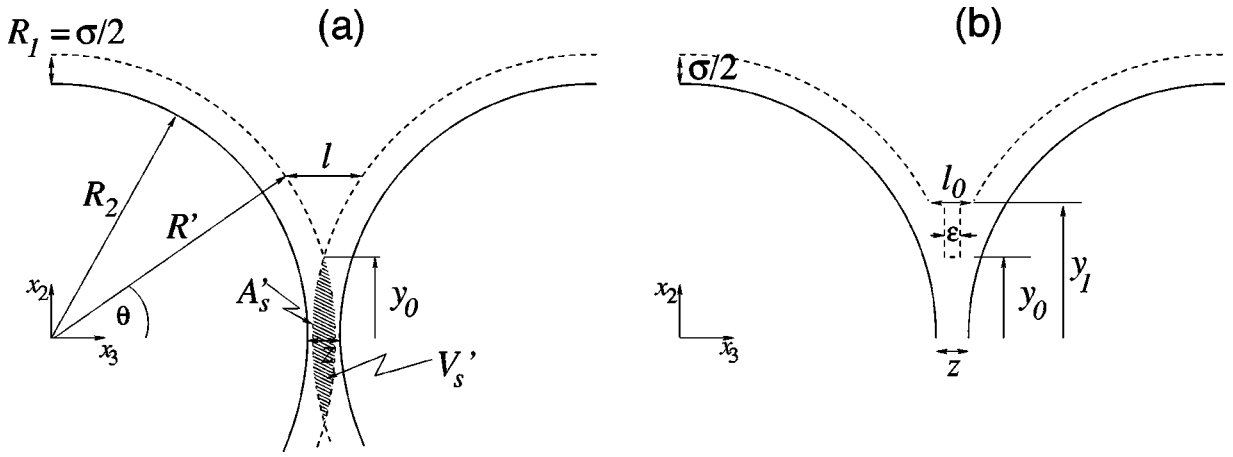

FIG. 2. (a) Geometrical definitions for two colloids in the depletion regime. The dashed lines indicate the surfaces of the exclusion spheres. Their overlap defines a volume V_s' and an overlap surface area A_s'. (b) Modeling the annular wedge part with widths $l<l_0$ by an annular slit of width ϵ in which the solvent gas is effectively two dimensional.

Here l is the horizontal distance between the two (exclusion) spheres corresponding to angle θ, see Fig. 2. For very large α, this approximation is certainly justified, since locally the geometry resembles the planar slit. Using

$$l = 2R' - 2x - (1-z), \tag{10}$$

$$\cos\theta = x/R', \tag{11}$$

we transform Eq. (8) into

$$F_\alpha(z) = \pi R' \int_{z-1}^{\infty} dl f_\infty(l). \tag{12}$$

The upper limit in this integral over the slit width has been replaced by infinity since it can be assumed that the solvation force approaches its limiting value $f_\infty(l\to\infty)=0$ when l is just a few σ, which should be considerably smaller than R'. Now the solvation force per unit area is defined by

$$f_\infty(l) = -\frac{d\gamma(l)}{dl}, \tag{13}$$

where $\gamma(l)$ is the excess grand potential (i.e., bulk grand potential subtracted) of the system of the two parallel walls which define the slit. Using the fact that $\gamma(\infty)=2\gamma_\infty$, where γ_∞ is the surface tension of a single hard wall in a sea of small spheres, we find

$$F_\alpha(z) = \pi R'[\gamma(z-1) - 2\gamma_\infty]. \tag{14}$$

If $z<1$ (i.e., no single small sphere fits into the slit) the planar slit surface tension arises from the release of free volume to the small spheres, $\gamma = p(z-1)$. Thus

$$F_\alpha(z) = \pi R'[p(z-1) - 2\gamma_\infty], \quad z \leqslant 1. \tag{15}$$

The depletion force is seen to depend only on the (hard-sphere) pressure p and surface tension γ_∞ for which we possess accurate approximations, see Eqs. (2) and (3).

B. Energy analysis

Following Henderson [8] we can arrive at the Derjaguin approximation also by an analysis of the grand potential which can be decomposed into a ''volume,'' a ''surface area,'' and a ''line'' term according to

$$\Omega(z) = -pV_s(z) + 2\pi R'^2 \int_{-1}^{1} d(\cos\theta)\,\gamma(l) \tag{16}$$

$$= -pV_s(z) + \gamma_\infty A_s(z) + \pi R' \int_0^\infty dl[\gamma(l) - 2\gamma_\infty]. \tag{17}$$

Here, V_s is the volume available to the small spheres [i.e., outside the two (possibly overlapping) exclusion spheres] A_s is the corresponding surface area of the two (possibly overlapping) exclusion spheres,

$$V_s(z) = V_0 - V_s' = V_0 - \frac{8}{3}\pi R'^3 + \frac{\pi}{2}(z-1)^2 \times\left(R' + \frac{z-1}{6}\right) \quad (z<1), \tag{18}$$

$$A_s(z) = A_0 - A_s' = 8\pi R'^2 + 2\pi R'(z-1) \quad (z<1) \tag{19}$$

(V_0 is the total system volume), and the last term is the ''line tension'' contribution *independent* of the length of the overlap circle $2\pi y_0$ and thus independent of z. Using

$$F_\alpha(z) = -\frac{\partial\Omega}{\partial z} \tag{20}$$

and retaining only the leading terms in $1/R'$, one arrives at the Derjaguin result, Eq. (15).

C. Statistical mechanical analysis

Summarizing Henderson's analysis, let us consider a fixed big sphere surrounded by a bath of small spheres. This sphere exerts an external, hard-body potential V_i^{ext} on small

spheres ($i=1$) and on any other large spheres ($i=2$). The work to insert another big sphere at distance z from the first sphere is given by $-c_2^{(1)}(z)$. Here, $c_2^{(1)}(z)$ is the one-body correlation function given by

$$c_2^{(1)}(z)=\ln[\rho_2(z)\Lambda_2^3]-\tilde{\mu}_2(z), \tag{21}$$

$$\tilde{\mu}_2(z)=\mu_2-V_2^{\mathrm{ext}}(z). \tag{22}$$

In these expressions, Λ_2 is the de Broglie wavelength of the big spheres and μ_2 is their chemical potential. For our configuration of interest, $\rho_2(z)$ is the one-body density profile of big spheres on another big sphere in the bath of small spheres *in the dilute limit* ($\mu_2\to-\infty$).

The first two equations in a hierarchy of functional derivatives of the grand potential are

$$\frac{\delta\Omega}{\delta\tilde{\mu}_i(\mathbf{x})}=-\rho_i(\mathbf{x}), \tag{23}$$

$$\frac{\delta^2\Omega}{\delta\tilde{\mu}_i(\mathbf{x})\,\delta\tilde{\mu}_j(\mathbf{y})}=-\{\rho_i(\mathbf{x})\rho_j(\mathbf{y})[g_{ij}(\mathbf{x},\mathbf{y})-1]+\rho_i(\mathbf{x})\,\delta^{(3)}(\mathbf{x}-\mathbf{y})\,\delta_{ij}\}. \tag{24}$$

Let us assume that the center of the first, fixed sphere defines the origin of the coordinate system, and the coordinates of the center of the second big sphere are given by $\mathbf{x}=\{x_1,x_2,x_3\}=\{0,0,2R_2+z\}$. Since the external potential V_2 vanishes for $z>0$ we find, using the above equations and the definition of the depletion force, Eq. (20),

$$F_\alpha(z)=c_2^{(1)\prime}(z)=\frac{\rho_2'(z)}{\rho_2(z)}\quad(z>0) \tag{25}$$

$$=\frac{1}{\rho_2(z)}\int d^3\mathbf{y}\sum_{i,j=1,2}\frac{\delta^2\Omega}{\delta\tilde{\mu}_i(\mathbf{x})\,\delta\tilde{\mu}_j(\mathbf{y})}\frac{\partial\tilde{\mu}_j(\mathbf{y})}{\partial y_3}. \tag{26}$$

In the dilute limit ($\rho_2\to0$) this expression simplifies to

$$F_\alpha(z)=-\int d^3\mathbf{y}\frac{\partial V_1^{\mathrm{ext}}(\mathbf{y})}{\partial y_3}\rho_1(\mathbf{y})[g_{12}(\mathbf{x},\mathbf{y})-1]. \tag{27}$$

By virtue of the derivative of the external potential V_1^{ext} (exerted by the fixed sphere on the small spheres) only the surface of the exclusion sphere (i.e., one of the dashed lines in Fig. 2) contributes to the integral. Since $\rho_1(\mathbf{y})$ is the density profile of small spheres around the fixed sphere, and $\rho_1(\mathbf{y})g_{12}(\mathbf{x},\mathbf{y})=\rho(\mathbf{y};\mathbf{0},\mathbf{x})$ is the density profile of small spheres around the fixed sphere but with the second sphere fixed at position $\mathbf{x}$, we recover Eq. (5):

$$F_\alpha(z)=2\pi R'^2\int_{-1}^{1}d(\cos\theta)\cos\theta[\rho(\{R',\theta\};\mathbf{0},\mathbf{x})-\rho_1(R')] \tag{28}$$

$$=2\pi R'^2\int_{-1}^{\cos\theta_{\min}}d(\cos\theta)\cos\theta\rho(\{R',\theta\};\mathbf{0},\mathbf{x}), \tag{29}$$

$$\cos\theta_{\min}=\begin{cases}1-(1-z)/(2R') & (z<1)\\ 1 & (z>1).\end{cases} \tag{30}$$

Although the integral in Eq. (5) extends over the whole surface of the big sphere, the contribution of surface elements with azimuthal angle $\theta<\theta_{\min}$ is zero since the density vanishes there.

To identify the Derjaguin limit it is useful to keep the second term in the brackets on the right-hand side (rhs) of Eq. (28) [writing for the contact density of small spheres at a single large sphere $\rho_s=\rho_1(R')$]:

$$F_\alpha(z<1)=2\pi R'^2\int_{-1}^{\cos\theta_{\min}}ada[\rho(\{R',a\};\mathbf{0},\mathbf{x})-\rho_s]+2\pi R'^2\rho_s\int_{-1}^{\cos\theta_{\min}}ada \tag{31}$$

$$=2\pi R'^2\int_{-1}^{\cos\theta_{\min}}ada[\rho(\{R',a\};\mathbf{0},\mathbf{x})-\rho_s]+\pi R'\rho_s(z-1)\left(1+\frac{z-1}{4R'}\right). \tag{32}$$

Changing integration variables from $a=\cos\theta$ to l according to Eqs. (10) and (11) and identifying the upper limit with infinity, we find

$$F_\alpha(z<1)=\pi\int_0^\infty dl[R'-(l+1-z)][\rho(\{R',l\};\mathbf{0},\mathbf{x})-\rho_s]+\pi R'\rho_s(z-1)\left(1+\frac{z-1}{4R'}\right). \tag{33}$$

The "microscopic" Derjaguin approximation consists in setting

$$\cos\theta[\rho(\{R',l\};\mathbf{0},\mathbf{x})-\rho_s]=\left(1-\frac{l+1-z}{2R'}\right)\times[\rho(\{R',l\};\mathbf{0},\mathbf{x})-\rho_s]\approx\rho_w(l)-\rho_w, \tag{34}$$

where $\rho_w(l)$ is the contact density at one wall in a planar slit of width l and ρ_w is the contact density at a single planar wall. From statistical mechanics we furthermore know [14,15]

$$\rho_w(l)-\rho_w=f_\infty(l)=-\frac{d\gamma(l)}{dl}, \tag{35}$$

$$\rho_s=p+\frac{2\gamma_{R'}}{R'}+\frac{d\gamma_{R'}}{dR'}. \tag{36}$$

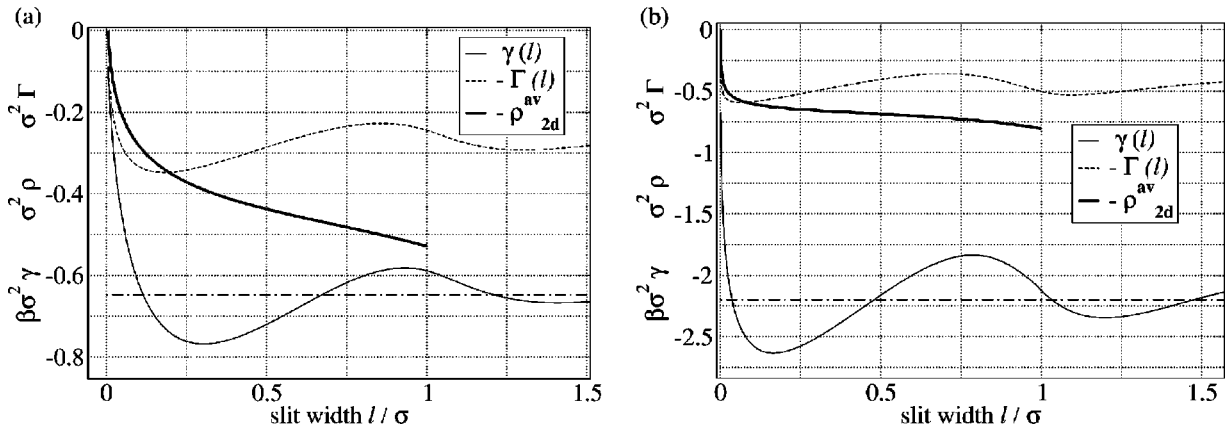

FIG. 3. Surface tension $\gamma(l)$ and the negative of the coverage $\Gamma(l)$ for planar slits of width l and two solvent densities: (a) $\rho=0.5$ and (b) $\rho=0.7$, as obtained from minimizing the Rosenfeld functional. The dot-dashed line shows the surface tension $\gamma(l\to\infty)=2\gamma_\infty$. The (negative of the) average density refers to the Derjaguin-like approximation of the 2D density in the annular wedge, Eq. (40).

Putting the last two equations into Eq. (33) we find the Derjaguin result as the leading order in R', and we can identify the finite-size correction of first order to it [the surface tension on the (exclusion) sphere with radius R', $\gamma_{R'}=\gamma_\infty+\delta/R'+\cdots$, thus $d\gamma_{R'}/dR'$ is negligible to first order in $1/R'$]:

$$F_\alpha(z<1)\approx F_\alpha^{\mathrm{Derjag}}+\pi R'\frac{2\gamma_\infty+\dfrac{z-1}{4}}{R'}(z-1). \qquad (37)$$

Interestingly, the finite-size corrections predict a smaller slope for the force curves ($\approx 10\%$ for $\alpha=10$) and a slight deviation from linearity which affects the curve only for $z\to 0$. We note that the considerations of Ref. [16] (their *wedge approximation*) would modify our finite-size corrections by $F_\alpha/(\pi R')\to F_\alpha/(\pi R')-\gamma_\infty/R'$, i.e., the slope corrections would be mitigated. In any case, the qualitative behavior for $z\to 1$ remains unchanged.

III. ANNULAR SLIT APPROXIMATION AND DERJAGUIN LIMIT

The microscopic Derjaguin approximation of Eq. (34) asserts that—apart from the geometrical factor $\cos\theta$—all annular wedges that are formed between the two large spheres for $z<1$ are equivalent, i.e., the contact value of the density on the spheres can be described by a single function, namely, $\rho_w(l)$. At first glance, there is a physical difference between these wedges: At $z=1$ the spheres on one "side" of the annular wedge can scatter with the spheres on the other side, as opposed to smaller values of z. Henderson argues that for small values of l, an effectively two-dimensional *ideal* gas of small spheres forms between the two colloids since the limiting three-dimensional density $\rho_w(l\to 0)$ stays *finite* and therefore an effective two-dimensional (2D) density $\rho_{2d}\approx l\rho_w$ *vanishes*. Therefore, scattering from one side of the wedge to the other should be negligible *unless* zero separation between the colloids occurs for radial distances $y_0<1/2$. Since $y_0^2\approx(1-z)R'$, it follows that the Derjaguin approximation should be valid for $z<1-1/(4R')$.

Is the concept of a nearly ideal 2D gas really valid in the annular wedge? For narrow slits with finite l we consider the small $l\ll\sigma$ expansion of $\rho_w(l)$ [14]:

$$\rho_w(l)=\frac{1}{\rho^{-1}\exp(-\mu^{\mathrm{ex}})+\pi l}. \qquad (38)$$

Here, μ^{ex} is the excess chemical potential of the small spheres and ρ the corresponding density. However, this limiting behavior is valid only for *very* small l. Rather one should study the effective 2D density in a slit defined by

$$\rho_{2d}^{\mathrm{slit}}(l)=\int_0^l dl'\,\rho(l')=\rho l+\Gamma(l), \qquad (39)$$

with $\Gamma(l)$ defining the coverage in the slit. A Derjaguin-like estimate for the average 2D density in the annular wedge up to a maximal parallel distance l_0 of the exclusion spheres follows

$$\rho_{2d}^{\mathrm{av}}(l_0)=\frac{1}{l_0}\int_0^{l_0}\rho_{2d}^{\mathrm{slit}}(l)=\frac{1}{l_0}\int_0^{l_0}\Gamma(l)dl+\frac{1}{2}\rho l_0. \qquad (40)$$

We can gain access to this quantity by using DFT again. As explained earlier, minimizing the Rosenfeld functional in the presence of an external field gives rather accurate density distributions. Carrying out the minimization in the presence of the two hard walls which define the slit gives us the explicit density distribution in the slit from which the surface tension γ, the coverage, and the average 2D density as functions of l can be calculated. The results for two medium densities are shown in Fig. 3. It is seen that the coverage and therefore also the average 2D density quickly reaches the level of $2\Gamma_\infty$ (twice the coverage on a single planar wall), and therefore the 2D gas between the spheres is far from ideal. We also notice that the surface tension $\gamma(l)$ falls quickly to $2\gamma_\infty$ and then shows moderate oscillations around that value.

Now, in order to formulate an alternative derivation of the Derjaguin limit we replace the last part of the annular wedge with $l<l_0$ by an annular slit of width $1+\epsilon$ where the spheres can only move perpendicular to the z axis, see the right panel of Fig. 2. The spheres in the slit can then be viewed as a system of hard disks. The surface tension in this fictitious slit is $\gamma(l_0)$ and its surface grand potential is written as

$$\Omega_{\rm sur}=\gamma(l_0)A_{\rm wed}+\sigma(y_0)2\pi y_0+\cdots, \tag{41}$$

where $A_{\rm wed}$ is the one-sided area of the wedge and we have introduced a line tension term $\sigma(y_0)$ which describes the interaction at the inner boundary of the wedge. Now for large R' we have

$$y_0\approx\sqrt{R'(1-z)}, \qquad A_{\rm wed}\approx A_0(y_1)+\pi R'(z-1), \tag{42}$$

where the area of a spherical cap is $A_0\approx\pi y_1^2$. Now the depletion force has three contributions:

$$F_\alpha(z<1)=\left(p+\frac{2\gamma_\infty}{R'}\right)\frac{dV_s}{dz}-\frac{d\Omega_{\rm sur}}{dz}+\int_{l_0}^{\infty}f_\infty(l)dl, \tag{43}$$

which arise since we have split the original Derjaguin integral, Eq. (12), according to $\int_{z-1}^{\infty}\cdots=\int_{z-1}^{0}\cdots+\int_0^{l_0}\cdots+\int_{l_0}^{\infty}\cdots$ and have incorporated the finite-size correction of Eq. (37). Simplifying Eq. (43) using the geometrical relations in Eq. (42) we find,

$$F_\alpha(z<1)=\pi R'\left[\left(p+\frac{2\gamma_\infty}{R'}\right)\left((z-1)+\frac{(z-1)^2}{4R'}\right)-\gamma(l_0)+\frac{\sigma(y_0)}{y_0}+\sigma'(y_0)-[2\gamma_\infty-\gamma(l_0)]\right]. \tag{44}$$

We have recovered the finite-size corrected Derjaguin result, Eq. (12), plus some line tension contribution. In view of the latter, Henderson's hypothesis of the equivalence of the annular wedges is based on the assumption that $\sigma(y_0)/y_0$ and $\sigma'(y_0)$ are insignificant for $y_0>1/2$. This is not trivial at all. Rather, if $\sigma(y_0)$ or $\sigma'(y_0)$ go to a finite value as $y_0\to 0$ we would expect the Derjaguin limit to fail for $z\to 1$.

The effective 2D gas in the annular slit

We can gain access to the line tension function $\sigma(y_0)$ by exploiting the nature of the quasi-2D gas in the wedge. Since the small spheres can only move in the plane perpendicular to the axis joining the centers of the two colloids, we rewrite the surface grand potential of our fictitious slit as

$$\Omega_{\rm sur}\to\Omega_{\rm 2d}=-p_{\rm 2d}(\rho_{\rm 2d})A_{\rm wed}+\gamma_{\rm 2d}(\rho_{\rm 2d};y_0)2\pi y_0, \tag{45}$$

appropriate for the 2D volume and area grand potential contributions of a system of hard disks. Now let us think about what is physically happening when the second colloid approaches the first one at distances $z\leqslant 1$: A circular cavity forms in the center of the quasi-2D gas which cannot be reached by the centers of the solvent spheres. Therefore we can express the last equation as

$$\Omega_{\rm 2d}=-p_{\rm 2d}A_0(y_1)+\mu_{\rm cav}(y_0'). \tag{46}$$

Here, the first term is the z-independent 2D volume term [$A_0(y_1)\approx\pi y_1^2$, see the right panel of Fig. 2], and we have introduced $\mu_{\rm cav}(y_0')$, the work needed to create a cavity of radius y_0'. From the reasoning above we would expect that $y_0'=y_0$. However, in our calculations of surface tensions and coverages in slits (see Fig. 3) we have seen that for very small slit widths ($l<\delta$) $\rho_{\rm 2d}^{\rm av}\to 0$. The limiting distance δ can be estimated from the small l expansion of the contact density in slits, Eq. (38):

$$\delta(\rho)\approx\rho^{-1}\exp(-\mu^{\rm ex}). \tag{47}$$

This is indeed a small length compared to σ: $\delta(0.5)\approx 4\times 10^{-2}$, $\delta(0.7)\approx 1\times 10^{-3}$. But the depleted area in the annular wedge up to distances δ must be added to the cavity, and therefore

$$y_0'\approx\sqrt{R'[(1-z)+\delta]}. \tag{48}$$

The problem of the insertion energy of an additional cavity was the starting point of scaled particle theory; here we can use the two-dimensional version [17] to obtain

$$\mu_{\rm cav}(y_0')=\begin{cases}p_{\rm 2d}\pi y_0'^2+\gamma_{\rm 2d}2\pi y_0'+\epsilon_{\rm 2d} & (y_0'>1/2)\\ -\ln(1-\pi\rho_{\rm 2d}y_0'^2) & (y_0'<1/2)\end{cases} \tag{49}$$

$$p_{\rm 2d}=\frac{4}{\pi}\frac{\eta_{\rm 2d}}{(1-\eta_{\rm 2d})^2}, \tag{50}$$

$$\gamma_{\rm 2d}=-\frac{2}{\pi}\frac{\eta_{\rm 2d}^2}{(1-\eta_{\rm 2d})^2} \tag{51}$$

$$\epsilon_{\rm 2d}=-\eta_{\rm 2d}\frac{1-2\eta_{\rm 2d}}{(1-\eta_{\rm 2d})^2}-\ln(1-\eta_{\rm 2d}) \tag{52}$$

$$\left(\eta_{\rm 2d}=\frac{\pi}{4}\rho_{\rm 2d}\right). \tag{53}$$

The contact to the original surface energy of the slit, Eq. (41), is made by setting $\gamma(l_0)=-p_{\rm 2d}$, thus it follows that $\sigma(y_0)\to\gamma_{\rm 2d}$. To obtain numbers, we simply choose l_0 such that $\gamma(l_0)=2\gamma_\infty$. Using Eq. (3) for the 3D surface tension, we can determine $\rho_{\rm 2d}$ as a function of ρ, the 3D density of small spheres. Remember that physically it would be also quite sensible to identify the 2D density via Eq. (39), $\rho_{\rm 2d}=\rho_{\rm 2d}^{\rm av}$. A quick glance at Fig. 3 assures us that the two definitions of $\rho_{\rm 2d}$ are quite consistent with each other [18].

One might be concerned that the validity of Eq. (49) is limited for intermediate disk sizes $y_0'=1,\ldots,2$ (where we would need it if calculating numbers for $\alpha=10$, say) as

scaled particle theory is by construction only an interpolation between the known analytical behavior of $\mu_{\mathrm{cav}}(y_0')$ for $y_0' < 1/2$ on the one side and $y_0' \to \infty$ on the other side. In view of lack of appropriate data in the literature we have performed a quick MC check for two densities $\rho_{2\mathrm{d}} = 0.4$ and 0.6, the results are shown in Appendix A. From these results it follows that scaled particle theory is precise enough for our purposes.

The final result for the depletion force, following from Eqs. (43) and (44) and the considerations of the previous paragraphs, takes the following form:

$$\frac{F_\alpha(z<1)}{\pi R'} = \frac{1}{\pi R'}\left(p + \frac{2\gamma_\infty}{R'}\right)\frac{dV_s}{dz} - \frac{1}{\pi R'}\frac{d\mu_{\mathrm{cav}}}{dz} \tag{54}$$

$$= \left(p + \frac{2\gamma_\infty}{R'}\right)\left((z-1) + \frac{(z-1)^2}{4R'}\right) + \begin{cases} \rho_{2\mathrm{d}} \dfrac{1 - \dfrac{1-z+\delta}{2R'}}{1 - \pi\rho_{2\mathrm{d}} y_0'^2} & (y_0' < 1/2) \\ \left(p_{2\mathrm{d}} + \dfrac{\gamma_{2\mathrm{d}}}{y_0'}\right)\left(1 - \dfrac{1-z+\delta}{2R'}\right) & (y_0' > 1/2), \end{cases} \tag{55}$$

$$y_0' = \sqrt{(1-z+\delta)\left(R' - \frac{1-z+\delta}{4}\right)}. \tag{56}$$

Here, for the sake of completeness, the exact geometrical expression for the cavity radius y_0' is given. The expression in Eq. (48) is the leading term in an expansion of y_0' with respect to R'. Before we perform a quantitative comparison of Eq. (55) to available simulation and DFT data, let us appreciate the difference between the Derjaguin limit and this result by selecting $y_0' = 1/2$. For large enough R', $z \approx 1$ and the Derjaguin force is approximately $-2\gamma_\infty$. On the other hand, for the annular slit approximation most of the terms in Eq. (55) drop out and using Eqs. (50) and (51) we find the force $-2\gamma_\infty(1-\eta_{2\mathrm{d}})$. Thus we see that the Derjaguin force is corrected by a multiplicative factor which is notably different from unity since $\eta_{2\mathrm{d}} \gtrsim \eta_{3\mathrm{d}} = \pi/6\rho$. This is the key difference to the considerations in Ref. [8] where $\eta_{2\mathrm{d}}$ was estimated to be close to zero. Note, however, that the actual *number* of particles in the annular slit is small for moderate size ratios α, see Eq. (57) below.

IV. RESULTS FROM THE ANNULAR SLIT APPROXIMATION AND COMPARISON WITH DFT AND MD

Having obtained a closed expression for the force in the depletion region, Eq. (55), we can compare results to the available MD data and to the DFT results. Instead of using the results from Ref. [5] we apply the bridge functional formalism of Ref. [19] to obtain results which are "one test-particle consistent." In effect, the equations for the depletion potential are transformed into RHNC-type equations where Rosenfeld's density functional (or extensions thereof) is the generating source for the bridge diagrams. For more details we refer to Appendix B where we have outlined the procedure and compared it to the previous DFT results. Summarizing the results from Appendix B, the self-consistency for one test particle gives a relatively small shift of the depletion force for $z < 0.6$–0.7 which is always upwards. This adds up to a 10–20 % correction upwards for the depletion potential at contact, $W_\alpha(z=0)$. For $z > 0.7$, the results are *quantitatively almost unchanged*. Especially the failure of the previous results to converge to the Derjaguin limit remains unaltered.

For the largest ratio $\alpha = 10$ where simulation data are available, we show results for the depletion force in Fig. 4. Values for the force at $z = 1$ are compared in Table I. In general, the agreement between the simulations and our annular slit approximation is surprisingly good. The approximation follows the trend of the simulation data to produce a maximum in the depletion force for $z < 1$ and $\rho > 0.5$. A pronounced maximum is absent in the DFT results for the densities shown. Despite the better agreement of the annular slit approximation with the simulation data, it is hard to tell whether for this size ratio α there is already a serious problem with DFT. First, there are no error bar estimates for the MD data available, and second, the approximation suffers from possible errors due to a finite number of particles in our idealized annular slit. This number can be estimated by

$$N_s = \rho_{2\mathrm{d}} A_{\mathrm{wed}} \approx \rho_{2\mathrm{d}} \pi R' l_0. \tag{57}$$

Indeed, since $l_0 \approx 0.2$–0.4 (see Fig. 3) $N_s < 5$ for all densities ($\alpha = 10$) According to this estimate, our considerations should become increasingly reliable for larger $\rho_{2\mathrm{d}}$ and larger α.

For larger α, the discrepancy between the annular slit approximation and the DFT results becomes striking. We show this in Fig. 5 for two size ratios $\alpha = 10$ and $\alpha = 100$. As we have explained, the annular slit approximation can be expected to become more accurate for larger α and it has the correct limiting behavior, so the conclusion would be that DFT becomes increasingly unreliable for $\alpha > 10$. Although not shown in the figure, there is already a substantial difference for $\alpha = 20$, say. Thus one should regard with extreme caution the claim in Ref. [5] that insertion route DFT can be expected to be rather accurate also for size ratios larger than 10. A similar claim made about a bridge diagram improved HNC treatment of the depletion potential (see Ref. [4]) should also be treated with caution as the HNC results show similar defects as the DFT results. Recall that the improved, test-particle consistent DFT results shown here can be viewed as HNC results with bridge diagram corrections supplied by the density functional and both methods can be formulated in the language of insertion route DFT.

Finally we calculate the quantity $W_\alpha(0) - W_\alpha(1)$ (for $\alpha = 10$) which is roughly the depletion potential difference between colloid contact and the first minimum for medium to

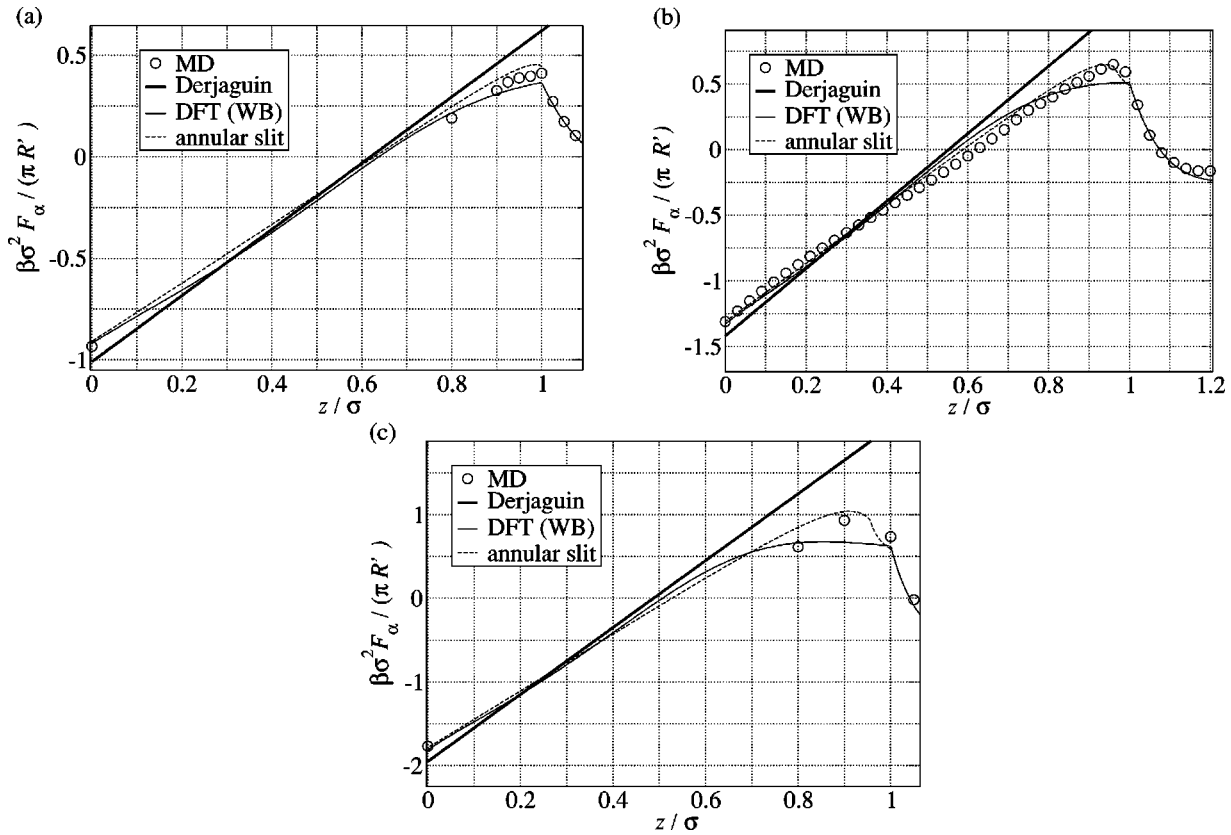

FIG. 4. The scaled force between two colloidal particles in the depletion region $z<1$ for a size ratio $\alpha=10$ and for three solvent densities: (a) $\rho=0.5$, (b) $\rho=0.6$, and (c) $\rho=0.7$. Comparison between the annular slit approximation [Eq. (55)], MD data [3], and test-particle consistent DFT based on the White Bear (WB) functional. The small differences between results obtained with the Rosenfeld and the White Bear functional are discussed in Appendix B, see Fig. 7 and the subsequent discussion.

high densities. The results are collected in Table II. We see that the previous DFT results predict that the potential at colloid contact is minimal for all values of ρ. This finding is not changed by imposing test-particle consistency; only the absolute value of the potential difference is reduced somewhat. The annular slit approximation predicts that the absolute minimum jumps to $z\approx 1$ for $\rho\approx 0.83$, still far away from the Derjaguin value 0.68. For $\alpha=100$, however, the jump of

TABLE I. Results for the scaled depletion force at $z=1$, $F_\alpha/(\pi R')$, for the annular slit approximation, from MD simulations [3], test-particle consistent DFT, and the Derjaguin approximation ($\alpha=10$). Note that the annular slit approximation predicts that the value of the scaled force at this point is essentially given by ρ_{2d}, the effective 2D density.

			$\frac{F_\alpha(z=1)}{\pi R'}$			
ρ	ρ_{2d}	δ	Eq. (55)	MD	DFT	Derjag.
0.4	0.22	0.18	0.28	0.22	0.22	0.31
0.5	0.34	0.04	0.44	0.41	0.36	0.62
0.6	0.46	$8\cdot10^{-3}$	0.49	0.57	0.51	1.15
0.7	0.59	$1\cdot10^{-3}$	0.60	0.74	0.62	2.05
0.8	0.71	$5\cdot10^{-5}$	0.71		0.64	3.55
0.9	0.81	$8\cdot10^{-7}$	0.81		0.62	6.01

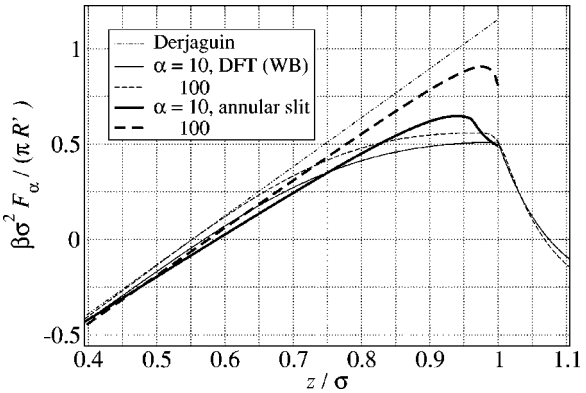

FIG. 5. Scaled depletion force for size ratios $\alpha=10$ and $\alpha=100$: Comparison between the annular slit approximation (gray curves) and test-particle improved DFT based on the White Bear (WB) functional. The solvent density is $\rho=0.6$. Note that the annular slit approximation approaches the Derjaguin limit quite slowly, nevertheless the Derjaguin limit is not reached at all by the DFT results.

TABLE II. Depletion potential difference $W_\alpha(0)-W_\alpha(1)=\int_0^1 F_\alpha(z)dz$ ($\alpha=10$) calculated using insertion route DFT [5], test-particle improved DFT based on the White Bear functional, the annular slit approximation, and the Derjaguin approximation.

	$W_\alpha(0)-W_\alpha(1)$			
ρ	DFT [5]	Test-particle improved DFT	Annular slit approximation	Derjaguin
0.4	−3.65	−3.50	−3.15	−3.30
0.5	−4.32	−4.01	−3.46	−3.35
0.6	−4.69	−4.16	−3.50	−2.27
0.7	−4.70	−3.84	−2.89	0.87
0.8	−4.39	−3.19	−1.02	7.79
0.9	−3.77	−2.38	3.12	21.64

the absolute minimum occurs at a density of 0.73, according to the annular slit approximation.

V. SUMMARY AND CONCLUSIONS

In this paper, we have analyzed the depletion force between hard colloids in a solvent consisting of small hard spheres. We started from an already previously observed disagreement between simulation data/results from Rosenfeld's DFT and the Derjaguin limit. Albeit first derived on purely phenomenological grounds, equilibrium statistical mechanics strongly supports the validity of the Derjaguin limit for large size ratios α between colloids and solvent spheres. The disagreement between simulation data/DFT and the Derjaguin limit in the depletion zone for $\alpha=10$ could be explained by an effective approximation which analyzes the structure of the solvent between the two colloids in terms of a (fairly) dense 2D gas of hard disks. The depletion force near the onset of the depletion zone (i.e., where exactly one solvent sphere fits between the colloids) is mainly determined by the force to create a disk cavity in the effective 2D gas. Requiring the Derjaguin limit for $\alpha\to\infty$, there are no free parameters for the 2D gas. The agreement with simulation data is very good even at the relatively small size ratio $\alpha=10$.

For higher size ratios $\alpha>10$ no simulation data are available, and existing DFT results showed no convergence towards the Derjaguin limit. Imposing test-particle consistency we calculated improved DFT results which however did not alter their large α behavior. Already for $\alpha=20$ the disagreement of the DFT depletion force with the results of the effective annular slit approximation becomes pronounced, especially in the region $z>0.7\sigma-0.8\sigma$. Also a small, but systematic deviation from linearity as $z\to0$ remains in the DFT results for an increasing size ratio α. We conclude that the limit of reliability of insertion route DFT is reached for $\alpha=10$. Through the test-particle consistent calculations we have shown that insertion route DFT and integral equation approaches are methodologically equivalent to each other; the single variants differ in their choice for the bridge functional. Similar limits for the reliability can therefore be also expected for integral equations. Likewise a similar limit will apply if one treats solvophobic colloids in attractive fluids with repulsive cores using Rosenfeld's DFT for hard sphere reference systems. To reach larger size ratios, the analysis of the annular slit approximation could also be extended to this case.

We have shown that quite subtle packing effects between the colloids play a role in determining the depletion force for medium to large size ratios. In light of this it is actually amazing that insertion route DFT (which explicitly needs only the density distribution around *one* colloid) captures most of the effects and only misses the intricate effect of the quasi-2D gas. We emphasize again that the insertion procedure is formally exact but we possess only approximate expressions for the hard sphere density functional whose functional derivative is needed for the insertion procedure to work. The two variants investigated herein, the Rosenfeld and the White Bear functional, are—despite being very precise—not exact. One deficiency, if not the main, lies in the bulk direct correlation functions $c^{(n)}$ of order $n\geqslant2$: they are zero outside the hard core according to the functionals, but from simulations and integral equations we know otherwise. Requiring test particle consistency has fixed this shortcoming for $c^{(2)}$, but for all higher-order ($n>2$) correlation functions one should require consistency for $n-1$ fixed test-particles. Part of the problem for $n=3$ is thus the determination of the density profile with the two colloids fixed. Therefore, it would be interesting to see how brute force DFT fares for size ratios $\alpha>10$, i.e., whether one could observe the oscillatory packing in the annular wedge directly and how it is related to $c^{(3)}$.

Throughout the paper we have argued that the Derjaguin limit for the depletion force is meaningful. The annular slit approximation, Eq. (55), predicts the leading correction to the force $\propto\alpha^{-1/2}$. Interesting enough, this is a nonanalytic term but the Derjaguin limit is still reached continuously in the variable $1/\alpha$. Since the depletion force is also connected to an integral over the surface densities, Eq. (5), this constitutes a hint that the density profile also contains nonanalytic contributions in $1/\alpha$. In fact, whereas there are good arguments that the density profile around hard convex objects should have an analytic expansion in terms of the curvatures [20], such an analyticity requirement does not hold for profiles around nonconvex objects (such as the two-colloid configuration in the depletion region). Consequently, there is the possibility that for $1/\alpha\to0$ the surface densities do not reach the Derjaguin limit of the surface densities in a planar slit configuration, Eq. (38). Possible singular contributions can not be understood with the current theories due to entropic arguments. A finite difference between the surface density and its Derjaguin limit would also constitute a surprise since it would point to small sphere correlations which are much larger than the bulk correlation length and allude to a phase transition such as solidification between the spheres for which there are no hints. Nevertheless the nonanalyticity of density profiles around curved objects is an extremely interesting subject in itself which is currently being explored [21].

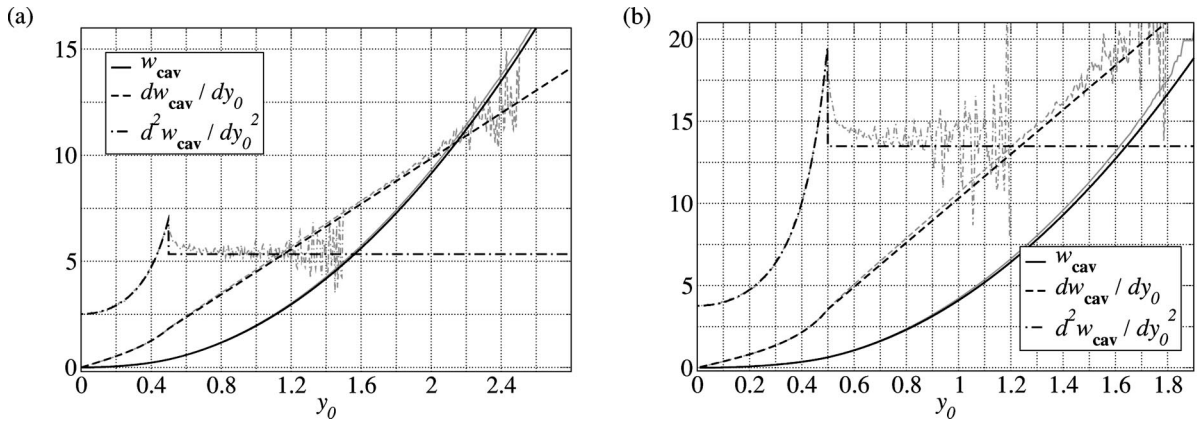

FIG. 6. Monte Carlo results for the insertion energy (and its first two derivatives) of an (exclusion) disk of radius y_0 into a system of hard disks with diameter 1. The thick black lines are the scaled particle predictions, the broken gray lines are raw data. The disk densities are (a) $\rho_{2d}=0.4$ and (b) $\rho_{2d}=0.6$.

ACKNOWLEDGMENTS

The author wants to thank R. Evans, R. Roth, and S. Dietrich for enlightening discussions on the subject and a careful reading of the manuscript.

APPENDIX A: QUALITY OF SCALED PARTICLE THEORY FOR HARD DISKS IN 2D

To check the reliability of the 2D scaled particle theory predictions for the insertion energy of a cavity with radius y_0, $w_{cav}(y_0)$, we performed Monte Carlo tests for two medium densities, $\rho_{2d}=0.4$ and $\rho_{2d}=0.6$. The insertion energy is given by

$$w_{cav}(y_0)=\ln p_0(y_0), \tag{A1}$$

where $p_0(y_0)$ is the probability to find no center of a disk within a circle of radius y_0 around an arbitrary point. Therefore we chose for each Monte Carlo move a new, random point, around which we checked the latter condition [22]. The results, obtained for 4000 disks and roughly 10^8 moves, are depicted in Fig. 6. The MC results are compared to scaled particle theory, and it is found that its simple prediction

$$w_{cav}(y_0)=\pi y_0^2 p_{2d}+2\pi y_0 \gamma_{2d} \tag{A2}$$

with γ_{2d} *independent* of the cavity radius is good except in the vicinity of $y_0=1/2$. At this point, exact analysis [17] demands that the third derivative has a singularity [23],

$$\frac{d^3 w_{cav}}{dy_0^3}(y_0 \to 1/2_+) \propto (y_0-1/2)^{-1/2}. \tag{A3}$$

This leads to a square-root-like cusp in the second derivative as can be seen in the MC results. Scaled particle theory ignores this cusp which is not too bad an approximation since the cusp quickly relaxes to a constant which is the pressure of the disk system. Apart from this effect of the nonanalyticity of w_{cav}, scaled particle theory is sufficiently precise for our purposes.

APPENDIX B: TEST-PARTICLE CONSISTENT DFT

In this section we shortly explain the route taken by Ref. [5] for obtaining the depletion potential, and introduce corrections thereto by requiring test-particle consistency. Numerical results for both methods are presented. Throughout this section $\beta=\sigma=1$.

Suppose we have a mixture of two hard species with particle radii R_1 and R_2. Species 2 refers to the colloids and the mutual interaction potentials are given by $u_{ij}(r)$. We split the density functional describing the mixture into an ideal gas and an excess part,

$$\mathcal{F}[\{\rho_i(\mathbf{r})\}]=\mathcal{F}_{id}[\{\rho_i(\mathbf{r})\}]+\mathcal{F}_{ex}[\{\rho_i(\mathbf{r})\}]. \tag{B1}$$

The hierarchy of direct correlation functions is defined as

$$c^{(n)}_{i_1,\ldots,i_n}(\mathbf{x}_1,\ldots,\mathbf{x}_n)=-\frac{\delta^{(n)}\mathcal{F}_{ex}}{\delta\rho_{i_1}(\mathbf{x}_1)\cdots\delta\rho_{i_n}(\mathbf{x}_n)}. \tag{B2}$$

Specifically for $n=1$ one can introduce an excess chemical potential functional,

$$\mu_i^{ex}[\mathbf{x};\{\rho_i(\mathbf{r})\}]=-c_i^{(1)}(\mathbf{x}), \tag{B3}$$

which reduces to the usual excess chemical potential if the densities are constant, $\mu_i^{ex}[\mathbf{x};\{\rho_i(\mathbf{r})=\text{const}\}]=\mu_i^{ex}(\{\rho_{i,0}\})$.

Suppose we have an inhomogeneous situation where one colloid is fixed. The depletion potential is then defined as the difference between the work needed to put another colloid particle into the system at position $\mathbf{x}$ on the one hand and at infinity on the other hand. Using the potential distribution theorem [24] we find

$$W_\alpha(x)=\lim_{\rho_2\to 0}(\mu_2^{ex}[\mathbf{x};\{\rho_i(\mathbf{r})\}]-\mu_2^{ex}(\{\rho_{i,0}\})), \tag{B4}$$

where we have assumed that $\lim_{|\mathbf{x}|\to\infty}\rho_1(\mathbf{x})=\rho_{1,0}$. Note that $\mu_2^{ex}[\cdots]$ depends in the required limit only on the density distribution $\rho_1(r)$ of species 1 around the colloid, i.e., *before* the second colloid is inserted. With a given excess functional

at hand, the depletion potential is found by obtaining $\rho_1(r)$ through grand potential minimization,

$$0=\frac{\delta F}{\delta\rho_i(\mathbf{x})}-\mu_i+V_i(\mathbf{x}) \tag{B5}$$

$$\rightarrow -\ln[\rho_1(\mathbf{x})]=\mu_1^{\mathrm{ex}}[\mathbf{x};\{\rho_1(\mathbf{x}'),0\}]-\mu_1^{\mathrm{ex}}(\{\rho_{1,0},0\})+u_{12}(\mathbf{x}), \tag{B6}$$

and then inserting this solution into Eq. (B4).

Test-particle consistency

The depletion potential is the negative potential of mean force between a pair of colloids at infinite dilution. The following relation is valid:

$$W_\alpha(|\mathbf{x}|)=-\ln g_{22}(|\mathbf{x}|;\{\rho_{1,0},0\})-u_{22}(|\mathbf{x}|), \tag{B7}$$

where g_{22} is the colloid-colloid distribution function in the limit of vanishing colloid density. On the one hand, this distribution function can be determined via the depletion potential described in the manner above. On the other hand, the excess functional defines the second-order correlation function $c_{ij}^{(2)}$ through Eq. (B2) (for $n=2$) which in turn can be inverted to give g_{ij} using the Ornstein-Zernike relation:

$$h_{ij}(|\mathbf{r}|)-c_{ij}^{(2)}(|\mathbf{r}|)=\sum_k \rho_{k,0}h_{ik}*c_{kj}^{(2)}(|\mathbf{r}|), \tag{B8}$$

$$h_{ij}(|\mathbf{r}|)=g_{ij}(|\mathbf{r}|)-1, \tag{B9}$$

$$h_{ik}*c_{kj}^{(2)}(|\mathbf{r}|)=\int d^3\mathbf{r}'h_{ik}(|\mathbf{r}'|)c_{kj}^{(2)}(|\mathbf{r}-\mathbf{r}'|). \tag{B10}$$

In general, both routes will give different results for an approximated free-energy functional.

To make both routes consistent with each other, we proceed as follows [19]: Consider the equation which relates the bridge function b_{ij} to the distribution and direct correlation function,

$$b_{ij}(|\mathbf{r}|)=-\ln g_{ij}(|\mathbf{r}|)-u_{ij}(|\mathbf{r}|)+\sum_k \rho_{k,0}h_{ik}*c_{kj}^{(2)}(|\mathbf{r}|). \tag{B11}$$

The various closures of integral equations follow by specifying a model for the bridge function, e.g., $b_{ij}(r)=0$ for the HNC closure. The bridge function can be generated by a bridge functional which we define to be the functional which contains all contributions beyond second order in a density expansion of the exact free-energy functional around fixed, constant bulk densities $\rho_{i,0}=\rho_i(\mathbf{r})-\Delta\rho_i(\mathbf{r})$:

$$\begin{aligned}\mathcal{F}[\{\rho_i(|\mathbf{r}|)\}]=&\mathcal{F}_{\mathrm{id}}[\{\rho_k(|\mathbf{r}|)\}]+F_{\mathrm{ex}}(\{\rho_{k,0}\})\\&+\mu_i^{\mathrm{ex}}(\{\rho_{k,0}\})\int d^3\mathbf{r}\Delta\rho_i(\mathbf{r})\\&-\frac{1}{2}\int d^3\mathbf{r}\int d^3\mathbf{r}'c_{ij}^{(2)}(\mathbf{r},\mathbf{r}';\mathrm{bulk})\\&\times\Delta\rho_i(\mathbf{r})\Delta\rho_j(\mathbf{r}')+\mathcal{F}_{\mathrm{ex}}^{\mathrm{br}}[\{\rho_k(\mathbf{r})\}].\end{aligned} \tag{B12}$$

Doubly occurring indices are summed over. To verify that the such introduced $\mathcal{F}_{\mathrm{ex}}^{\mathrm{br}}$ indeed generates the bridge functions, we minimize the grand potential according to Eq. (B5) in the presence of the interparticle potential, $V_i=u_{ij}$:

$$\frac{\delta\mathcal{F}_{\mathrm{ex}}^{\mathrm{br}}}{\delta\rho_i(\mathbf{r})}=-\ln\frac{\rho_i(\mathbf{r})}{\rho_{i,0}}-u_{ij}(\mathbf{r})+c_{ik}^{(2)}*\Delta\rho_k(\mathbf{r}). \tag{B13}$$

Since $\rho_{i,0}g_{ij}(|\mathbf{r}|)=\rho_i(|\mathbf{r}|)$ and $\rho_{i,0}h_{ij}(|\mathbf{r}|)=\Delta\rho_i(|\mathbf{r}|)$ we have recovered Eq. (B11) upon the identification

$$b_{ij}(\mathbf{r})=\frac{\delta\mathcal{F}_{\mathrm{ex}}^{\mathrm{br}}}{\delta\rho_i(\mathbf{r})}\Big|_{V_i=u_{ij}}. \tag{B14}$$

Up to now everything was exact but in order to specify a closure explicitly we assert that the true bridge functional can be approximated by the bridge functional of a reference model for which we possess an explicit form of $\mathcal{F}_{\mathrm{ex}}$:

$$\begin{aligned}\mathcal{F}_{\mathrm{ex}}^{\mathrm{br}}[\{\rho_k(\mathbf{r})\}]\approx&\mathcal{F}_{\mathrm{ex}}^{\mathrm{ref}}[\{\rho_k(\mathbf{r})\}]-\mu_i^{\mathrm{ex,\,ref}}(\{\rho_{k,0}\})\\&\times\int d^3\mathbf{r}\Delta\rho_i(\mathbf{r})+\frac{1}{2}\int d^3\mathbf{r}\int d^3\mathbf{r}'\\&\times c_{ij}^{(2),\mathrm{ref}}(\mathbf{r},\mathbf{r}';\mathrm{bulk})\Delta\rho_i(\mathbf{r})\Delta\rho_j(\mathbf{r}').\end{aligned} \tag{B15}$$

A remark is in order here. Note that Eqs. (B12) and (B15) together define a new functional which is now test-particle consistent, i.e., the inversion of the Ornstein-Zernike relation gives the same result as an explicit determination of the distribution functions through the density profiles around test particles. This consistency holds regardless of the form of the interparticle potential and of how good or bad the choice of the reference system is. Of course, the reference system of choice is again hard spheres described by Rosenfeld's functional [9] or a recently improved version, the White Bear functional [11].

In the limit $\rho_2\rightarrow 0$, relevant for the determination of the depletion potential, the equations for the distribution functions decouple. For g_{11} we have to solve the following equations ($r=|\mathbf{r}|$):

$$h_{11}(r)-c_{11}^{(2)}(r)=\rho_{1,0}h_{11}*c_{11}^{(2)}(r), \tag{B16}$$

$$\begin{aligned}-\ln g_{11}(r)-u_{11}(r)=&\rho_{1,0}h_{11}*(c_{11}^{(2),\mathrm{ref}}-c_{11}^{(2)})(r)\\&+(\mu_1^{\mathrm{ex,ref}}[r;\{\rho_{1,0}g_{11}(r),0\}]\\&-\mu_1^{\mathrm{ex,ref}}(\{\rho_{1,0},0\})).\end{aligned} \tag{B17}$$

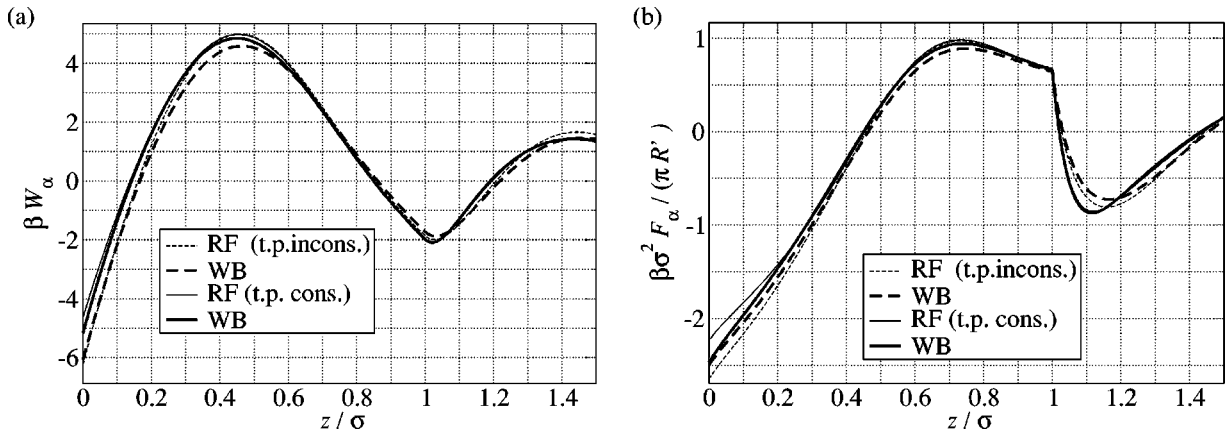

FIG. 7. (a) Depletion potential and (b) depletion force between two colloids for a solvent density of $\rho=0.8$ and a size ratio $\alpha=10$: Comparison between test-particle inconsistent and consistent results, using Rosenfeld's (RF) and the White Bear (WB) functional, respectively.

As expected, the colloids decouple and we are left with the equations for the one-component system. Employing the White Bear functional, we obtain one-component distribution functions which fit the MC data even better than the standard Verlet parametrization [25,26]. The input of h_{11}, c_{11} is needed to solve the next two equations for g_{12} (the normalized density distribution around one colloid):

$$h_{12}(r)-c_{12}^{(2)}(r)=\rho_{1,0}h_{11}{}^{*}c_{12}^{(2)}(r), \tag{B18}$$

$$-\ln g_{12}(r)-u_{12}(r)=\rho_{1,0}h_{12}{}^{*}(c_{11}^{(2),\mathrm{ref}}-c_{11}^{(2)})(r) + (\mu_1^{\mathrm{ex,ref}}[r;\{\rho_{1,0}g_{12}(r),0\}] - \mu_1^{\mathrm{ex,ref}}(\{\rho_{1,0},0\})). \tag{B19}$$

Having obtained h_{12}, c_{12}, the depletion potential is simply given by

$$W_\alpha(r)=-\ln g_{22}(r)-u_{22}(r)=\rho_{1,0}h_{12}{}^{*}(c_{12}^{(2),\mathrm{ref}}-c_{12}^{(2)})(r) + (\mu_2^{\mathrm{ex,ref}}[r;\{\rho_{1,0}g_{12}(r),0\}]-\mu_2^{\mathrm{ex,ref}}(\{\rho_{1,0},0\})). \tag{B20}$$

Comparing the expressions for the depletion potential for test-particle inconsistent and consistent DFT, Eqs. (B4) and (B20), we see that the main difference is buried in the first term on the rhs of Eq. (B20) since $\rho_1(r)|_{\mathrm{inconsistent}} \approx \rho_{1,0}g_{12}(r)|_{\mathrm{consistent}}$.

Results for the size ratio $\alpha=10$ reveal no huge differences between the test-particle consistent and inconsistent calculations. For distances between the colloids $z<0.6$–0.7 the consistent results give a somewhat higher force than the inconsistent results which adds up to a noticeable upward shift in $W_\alpha(z=0)$. Close to $z=0$ (contact), all routes show deviations from linearity which is predicted by the Derjaguin analysis. The test-particle consistent White Bear result have the smallest deviation which could be expected from previous articles [11,12] which report improved contact values for density profiles in the vicinity of hard objects. We note that these deviations from linearity remain as when α is increased up to 100. Apart from that the differences are minimal, even at higher densities. For $\rho_{1,0}=0.8$, we show the depletion potential and force in Fig. 7, calculated with the Rosenfeld and the White Bear functional.

Due to the accuracy in the one-component case, this choice of reference system has been extended to binary soft systems [28]. Again, the agreement with simulation data is extremely good but the size ratio in the binary systems was well below 10. Only recently the depletion potential between soft colloids in soft fluids has been calculated for size ratios of about 10 using this method [13]. In general, test-particle consistent DFT fares much better than any other theoretical method compared to the simulation data. Nevertheless, in the case of hard colloids in a Lennard-Jones fluid discrepancies to the simulation data occur which show the same footprints as the deviations we observe here in the case of hard colloids in hard fluids.

[1] N.F. Carnahan and K.E. Starling, J. Chem. Phys. **51**, 635 (1969).
[2] D. Henderson and M. Plischke, Proc. R. Soc. London, Ser. A **410**, 409 (1987).
[3] T. Biben, P. Bladon, and D. Frenkel, J. Phys.: Condens. Matter **8**, 10799 (1996).
[4] R. Dickman, P. Attard, and V. Simonian, J. Chem. Phys. **107**, 205 (1997).
[5] R. Roth, R. Evans, and S. Dietrich, Phys. Rev. E **62**, 5360 (2000).
[6] S. Melchionna and J.-P. Hansen, Phys. Chem. Chem. Phys. **2**, 3465 (2000).
[7] D. Goulding and S. Melchionna, Phys. Rev. E **64**, 011403 (2001).
[8] J.R. Henderson, Physica A **313**, 321 (2002).
[9] Y. Rosenfeld, Phys. Rev. Lett. **63**, 980 (1989).
[10] E. Kierlik and M.L. Rosinberg, Phys. Rev. A **42**, 3382 (1990).
[11] R. Roth, R. Evans, A. Lang, and G. Kahl, J. Phys.: Condens.

Matter **14**, 12 063 (2002).
[12] P. Bryk, R. Roth, M. Schoen, and S. Dietrich, Europhys. Lett. **63**, 233 (2003).
[13] S. Amokrane and J.G. Malherbe, J. Phys.: Condens. Matter **13**, 7199 (2001).
[14] J.R. Henderson, Mol. Phys. **59**, 89 (1986).
[15] J. R. Henderson, in *Fluid Interfacial Phenomena*, edited by C. A. Croxton (Wiley, New York, 1986), p. 555.
[16] B. Götzelmann, R. Evans, and S. Dietrich, Phys. Rev. E **57**, 6785 (1998).
[17] E. Helfand, H.L. Frisch, and J.L. Lebowitz, J. Chem. Phys. **34**, 1037 (1961).
[18] From $2\gamma_\infty(\rho) = -p_{2\mathrm{d}}(\rho_{2\mathrm{d}})$ it follows that $\rho_{2\mathrm{d}} = 0.33$ for $\rho = 0.5$ and $\rho_{2\mathrm{d}} = 0.59$ for $\rho = 0.7$.
[19] Y. Rosenfeld, J. Chem. Phys. **98**, 8126 (1993).
[20] P. Bryk, R. Roth, K.R. Mecke, and S. Dietrich, Phys. Rev. E **68**, 031602 (2003).
[21] P. König, K. Mecke, and R. Roth (unpublished).
[22] D.J. Adams, Mol. Phys. **28**, 1241 (1974).
[23] In Ref. [17], this singularity is given as $\propto (y_0 - 1/2)^{-1}$ which must be a misprint.
[24] J.R. Henderson, Mol. Phys. **50**, 741 (1983).
[25] L. Verlet and J.-J. Weiss, Phys. Rev. A **5**, 939 (1972).
[26] There is a small error in Ref. [25]. The first-order estimate for the decay length of the oscillations, Eq. (2.17) in the paper, should be changed:

$$\mu d \approx \frac{24A/d}{\eta_W g_W(1,\eta_W)} \rightarrow \frac{24A/d}{\eta g(1,\eta)}.$$

The second-order correction becomes important for higher densities:

$$\mu d \approx \frac{24A/d}{\eta g(1,\eta) + 4(d_W^3 - 4 + 3/d_W) g'(1,\eta)}.$$

The error also appears in the widely used Ref. [27].
[27] J.-P. Hansen and I. R. McDonald, *Theory of Simple Liquids* (Academic, London, 1976), p. 387.
[28] G. Kahl, B. Bildstein, and Y. Rosenfeld, Phys. Rev. E **54**, 5391 (1996).